RA'EGA
O ESPAÇO GEOGRÁFICO EM ANÁLISE
https://revistas.ufpr.br/raega

ISSN eletrônico 2177-2738
RA'EGA, Curitiba, PR, V.58, p. 39 – 62, 12/2023
.http://dx.doi.org/10.5380/raega.v58i0.93465

Efeitos da correção atmosférica em imagens multiespectrais orbitais para estudos em corpos d'água interiores

Analysis of the effects of atmospheric correction on orbital images for studies in interior water bodies

Gabriella C. Segedi [*], Rejane E. Cicerelli [*], Tati de Almeida[*], Henrique Llacer Roig[*], Diogo Olivetti [*], Vicente Bernardi[**], Adriana Castreghini [***]

[*] University of Brasília, Institute of Geosciences, Graduate Program in Applied Geosciences and Geodynamics, Geoprocessing Laboratory/GeoLab, e-mails: gabriella.segedi@gmail.com ; rejaneig@unb.br; tati_almeida@unb.br; roig@unb.br; di_olivetti@gmail.com
** University of Brasília, Faculty UnB Planaltina, Geostatistics and Geodesy Laboratory. Email: bernardi.jve@gmail.com
*** Londrina State University, Geosciences Departament. Email: adrianacfp@uel.br .

http://dx.doi.org/10.5380/raega.v58i0.93465

Abstract

The water reservoirs, in addition to their significance in electricity generation, serve as vital resources for various other requirements of the population. Images from orbital sensors have been applied to complement the monitoring of these environments and thus overcome the deficiency of spatial and temporal coverage of traditional techniques. However, studies involving water quality are still a great challenge due to the low signal coming from the water body and the interference of external factors (or environmental factors). Image correction/improvement procedures are often proposed, mainly to reduce atmospheric interference. In this study the best available atmospheric correction techniques were evaluated in order to indicate the technique that most closely matches the spectral response of remotely sensed images obtained in the field. During the study six atmospheric correction algorithms were applied (FLAASH, Second simulation of a Satellite Signal in the Solar Spectrum (6S), L8SR, Aquatic Reflectance (NASA/USGS), ACOLITE and Sen2Cor) that, based on the statistical analysis of discriminant analysis and covariance, indicated the 6S for Landsat and Sentinel images and ACOLITE for Landsat images as the most accurate. Although 6S showed a response close to the reference data, low variability in spectral response was observed. For time series, ACOLITE showed better capacity to correct the data. The type of application is also a preponderant factor, since it was evident that the use of time series indicated a different atmospheric correction technique when compared to the analysis of the scenes individually.

Keywords:
Inland water bodies; Atmospheric correction; Landsat-8; Sentinel-2.

ISSN eletrônico 2177-2738
RA'EGA, Curitiba, PR, V.58, p. 39 – 62, 12/2023
http://dx.doi.org/10.5380/raega.v58i0.93465

Resumo

Os reservatórios hídricos além de serem importantes para a produção de energia elétrica, são recursos para outras necessidades da população. Imagens de sensores orbitais são aplicadas para complementar o monitoramento desses ambientes e assim suprir a deficiência de cobertura espacial e temporal das técnicas tradicionais. No entanto, estudos envolvendo análises de qualidade de água ainda são um grande desafio devido ao baixo sinal proveniente do corpo d'água e a interferência de fatores externos (ou fatores ambientais). Procedimentos de correção das imagens são propostos com frequência, principalmente para a redução da interferência atmosférica. Nesse estudo foram avaliadas as melhores técnicas de correção atmosférica disponíveis no intuito de indicar aquela técnica que mais se aproxima da resposta espectral de sensoriamento remoto obtida em campo. No decorrer do estudo foram aplicados seis algoritmos de correção atmosférica (FLAASH, Second simulation of a Satellite Signal in the Solar Spectrum (6S), L8SR, Aquatic Reflectance (NASA/ USGS), ACOLITE e Sen2Cor) que, a partir das análises estatísticas de análise discriminante e covariância apontaram os aplicativos 6S para imagens Landsat e Sentinel e o ACOLITE para imagens Landsat como os mais acurados. Embora o 6S tenha apresentado resposta próxima dos dados de referência, observou-se baixa variabilidade na resposta espectral. Para séries temporais, o ACOLITE apresentou maior capacidade de correção dos dados. O tipo de aplicação também é um fator preponderante, pois ficou evidente que o uso de series temporais indicou uma técnica de correção atmosférica diferente quando comparado com a análise das cenas de forma individual.

Palavras-chave:
Corpos d´água interiores, Correção Atmosférica, Landsat-8, Sentinel-2.

I. INTRODUCTION

Artificial reservoirs are recognized as a means of obtaining clean energy, human supply, irrigation, aquaculture, pisciculture, recreation, navigation, and cooling of industrial effluents, among other uses. The maintenance of water quality in these environments depends on a series of anthropogenic factors, such as urban occupation, agriculture, domestic and industrial effluents, flow, among others, and natural factors (climate, slope, vegetation, among others). Therefore, understanding the reservoir dynamics becomes essential to ensure water security in the region where the project is installed (GONZÁLEZ-MÁRQUEZ *et al.*, 2018).

Orbital sensor images have been applied to complement the monitoring of these environments and thus address the spatial and temporal coverage deficiencies of traditional techniques. However, studies involving water quality analyses of water bodies are still a major challenge due to the low signal from the water body and interference from external factors (or environmental factors) that affect images in different ways. Additionally, other effects may be added to the water surface, such as specular reflection (STEINMETZ *et al.*, 2011; HARMEL *et al.*, 2018), spectral mixing by neighboring targets (DE KEUKELAERE *et al.*, 2018), among others. Important issues such as sensor characteristics, spectral sensitivity in each band to achieve a good signal-to-noise ratio, and calibration between detectors must also be modeled (WARREN *et al.*, 2019; EUGENIO *et al.*, 2020).

ISSN eletrônico 2177-2738
RA'EGA, Curitiba, PR, V.58, p. 39 – 62, 12/2023
http://dx.doi.org/10.5380/raega.v58i0.93465

Indeed, many studies have improved and developed image correction techniques (BERNARDO *et al.*, 2017; WANG *et al.*, 2019; WARREN *et al.*, 2019). However, most algorithms for atmospheric correction (AC) were developed for satellite sensors with medium spatial (or low) resolution for oceans, limiting their applications for smaller and optically more complex inland waters (MÉLIN, 2022). In summary, a limiting factor in water quality monitoring, even today, is atmospheric correction; that is, if the method employed is of poor quality, any results derived from water reflectance are subject to significant uncertainties (WARREN *et al.*, 2019).

Studies addressing this issue either develop solutions for isolated water bodies or adapt atmospheric correction routines. There are also cases that handle data in highly eutrophied environments, where the signal intensity is primarily from Optically Active Components (OAC) (BERNARDO *et al.*, 2017; WANG *et al.*, 2019; WARREN *et al.*, 2019). For example, Eugenio *et al.* (2020) adjusted a radiative transfer model to estimate concentrations of Chlorophyll-a (Chla) using multispectral (Worldview satellite) and hyperspectral (drones and airborne) images. Despite the corrections made, the estimation of Chl-a concentration still showed a Root Mean Square Error (RMSE) of 3.49, which may be impractical for water bodies with trophic states better than mesotrophic. Therefore, accurate calibrations and corrections are necessary to account for the spectral response of sensors, viewing angles, solar illumination geometries, atmospheric effects, and solar brightness disturbances.

Thus, there is a need to enhance the understanding of the optical characteristics of different water bodies and eliminate the effects of absorption and scattering from atmospheric components, such as atmospheric molecules, aerosols, and cloud particles.

Therefore, this research aims to evaluate different atmospheric correction techniques on Landsat 8 OLI and Sentinel 2 MSI images in an oligotrophic tropical aquatic environment. Among the models chosen and tested in this work are FLAASH (Fast Line-of-sight Atmospheric Analysis of Spectral Hypercubes) (Anderson *et al.*, 2002a), 6S (Second Simulation of the Satellite Signal in the Solar Spectrum) (VERMOTE *et al.*, 2016), ACOLITE (Atmospheric Correction for OLI 'lite') (BERNSTEIN *et al.*, 2005), Sen2Cor (MAIN-KNORN *et al.*, 2017), L8SR (Landsat 8 Surface Reflectance Product), and Aquatic Reflectance (L8PAR) (OGASHAWARA *et al.*, 2020), whose spectral responses after corrections will be compared with spectral data obtained in the field. Through statistical clustering analyses, we expect to understand the signal reconstruction processes in the application of atmospheric correction.

ISSN eletrônico 2177-2738
RA'EGA, Curitiba, PR, V.58, p. 39 – 62, 12/2023
http://dx.doi.org/10.5380/raega.v58i0.93465

II. MATERIALS E METHODS

Paranoá Lake (Figure 1), created in 1960 along with the founding of Brasília, is surrounded by buildings and used for recreational activities. In 2016, the Federal District faced a water crisis due to a prolonged drought period that resulted in water rationing in the city due to the low levels of supply reservoirs. This highlighted the need to use water from Paranoá Lake for public supply (PASSOS *et al.*, 2020) (Figure 1).

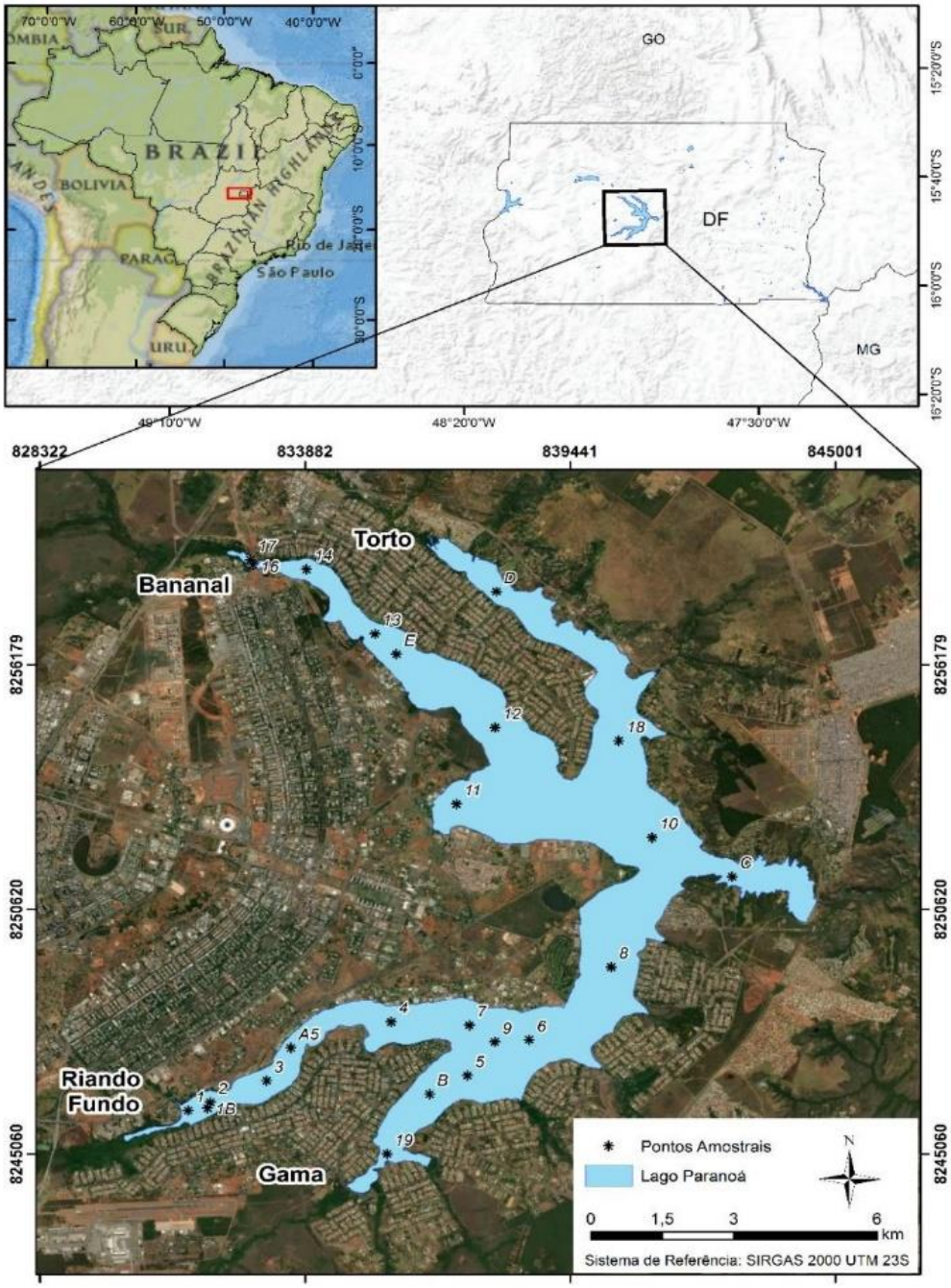

Figure 1 - Location of Paranoá Lake, Brasília/DF, containing the planned sampled fields (numbers) conducted in collaboration with the Companhia de Saneamento do Distrito Federal (CAESB) . (The authors, 2023)

ISSN eletrônico 2177-2738
RA'EGA, Curitiba, PR, V.58, p. 39 – 62, 12/2023
http://dx.doi.org/10.5380/raega.v58i0.93465

Currently, the water intake system for public supply from Paranoá Lake is implemented and operational, and constant and periodic monitoring of water quality becomes essential. The reservoir was selected as a case study because periodic limnological variable estimates indicated low concentrations, characterizing it as an oligotrophic water body (BATISTA; FONSECA, 2018). This characteristic aids in understanding the application of atmospheric correction algorithms, allowing the analysis of the variability of corrections in water reflectance data.

Remote sensing and limnological data acquisition

A total of four field campaigns were conducted (2020/08/17; 2020/10/04; 2017/05/05 and 2017/07/27), coinciding with the passage of Landsat 8 and Sentinel-2 satellites. On these days, (i) orbital images, (ii) field reflectance data, and (iii) limnological variables were acquired to assess water quality. The initial study methodology aimed to understand the complete hydrological cycle. However, due to logistical problems encountered with the need for equipment maintenance and calibration during the research development, as well as the pandemic, the four aforementioned collections were carried out.

Orbital images were preprocessed and obtained in the categories Provisional Landsat-8 Surface Reflectance Algorithm (L8SR) and L8PAR (Landsat-8 Provisional Aquatic Reflectance Product) for Landsat 8 OLI images, while for Sentinel-2 MSI, top-of-atmosphere reflectance (TOA) data were obtained.

For the acquisition of Remote Sensing Reflectance (R_{rs}) field data, a set of TriOS RAMSES spectroradiometers was used, with a wavelength range between 300nm and 950nm with measurements every 2.2nm. The radiometers were positioned following the methodology of radiometry outside the water to acquire water R_{rs} data and can be considered as ground truth for the reflectance values obtained by the applied atmospheric corrections. R_{rs} was calculated using the Mobley equation (1999).

$$R_{rs} = \frac{L_u - Ld * \rho}{E_d} \quad (1)$$

Where, L_u is the upward radiance of the water surface; Ld is the atmospheric radiance used to correct the effects of scattering and absorption of electromagnetic radiation in the air column; E_d is the downward irradiance on the water surface; ρ is a proportional factor dependent on sky conditions, wind speed, solar zenith angle, and viewing geometry, and using the suggested value of 0.028 for acquisition conditions, data for remote sensing reflectance (R_{rs}) were collected.

ISSN eletrônico 2177-2738
RA'EGA, Curitiba, PR, V.58, p. 39 – 62, 12/2023
http://dx.doi.org/10.5380/raega.v58i0.93465

Spectral curve measurements were obtained at approximately two-minute intervals at each collection point, generating a spectral curve every 10 seconds. Thus, the final spectral response product for each point is the average of the spectral curves generated within the collection time interval, allowing the calculation of surface reflectance individually using the MSDA_XE (Multi Sensor Data Acquisition System - Extended Edition) software and with the assistance of The R Project for Statistical Computing.

To align the RAMSES spectroradiometer (TriOS) data with the wavelength intervals of Landsat 8 OLI and Sentinel-2 MSI sensors, the Spectral Resampling tool in the Environment for Visualizing Images (ENVI) software was used.

Limnological data were collected using the EXO 2 multiparameter probe from the YSI manufacturer, providing information such as conductivity, dissolved oxygen (optical), Total Dissolved Solids (TDS), turbidity, hydrogen ion potential – pH, and water temperature.

Algorithms for Atmospheric Correction

In total, four atmospheric correction algorithms were compared for Landsat data: (i) FLAASH (Fast Line-of-sight Atmospheric Analysis of Spectral Hypercubes) (ANDERSON *et al.*, 2002b), (ii) 6S (Second Simulation of a Satellite Signal in the Solar Spectrum) (WANG *et al.*, 2018), (iii) ACOLITE (VANHELLEMONT; RUDDICK, 2015), in addition to reflectance images (iv) TOA (Top Of Atmosphere); (v) L8SR (Landsat 8 Surface Reflectance Product), and (vi) Aquatic Reflectance (L8PAR) (OGASHAWARA *et al.*, 2020).

For Sentinel images, the following atmospheric correction algorithms were compared: (i) FLAASH (Fast Line-of-sight Atmospheric Analysis of Spectral Hypercubes) (ANDERSON *et al.*, 2002b), (ii) 6S (Second Simulation of a Satellite Signal in the Solar Spectrum) (WANG *et al.*, 2018), (iii) ACOLITE (VANHELLEMONT; RUDDICK, 2015), (iv) Sen2Cor (MAIN-KNORN *et al.*, 2017), in addition to reflectance images (iv) TOA (Top Of Atmosphere).

The FLAASH algorithm (Fast Line-of-sight Atmospheric Analysis of Hypercubes) is based on the radiative transfer model. It corrects wavelengths in the visible region (380 to 760nm) through near-infrared (760 to 1200nm) and shortwave infrared (1200 to 3000nm) (COOLEY *et al.*, 2002). The 6S (Second Simulation of a Satellite Signal in the Solar Spectrum) is an enhancement of the 5S model, considering the effects of radiation in the atmosphere as a whole to eliminate the effects of Rayleigh scattering and aerosols, expanding the applications of this algorithm. It is one of the most widely used algorithms due to rigorous validations and elaborate radiative transfer codes (VERMOTE *et al.*, 2016). The ACOLITE atmospheric correction algorithm is a generic processor developed at RBINS (Belgian Institute of Natural Sciences) for atmospheric correction and

ISSN eletrônico 2177-2738
RA'EGA, Curitiba, PR, V.58, p. 39 – 62, 12/2023
http://dx.doi.org/10.5380/raega.v58i0.93465

processing for applications in coastal and inland waters, using dark spectrum adjustment for correction (VANHELLEMONT, 2020). This has been validated with surface data, mainly in the northern hemisphere (VANHELLEMONT, 2020).

The Provisional Landsat-8 Surface Reflectance Algorithm (L8SR) is the surface reflectance product generated from an atmospheric correction algorithm developed using the Second Simulation of the Satellite Signal in the Solar Spectrum Vectorial (6SV), refined to take advantage of OLI spectral bands with better radiometric resolution and signal-to-noise ratio. Additionally, the algorithm uses the new OLI Coastal aerosol band (0.433–0.450 µm), which is particularly useful for retrieving aerosol properties (VERMOTE *et al.*, 2016).

Aquatic Reflectance (AR) is a product provided by the United States Geological Survey (USGS) since April 1, 2020, known as L8PAR (Landsat 8 Provisional Aquatic Reflectance). This product calculates aquatic reflectance divided by π for R_{rs} calculation. The product is based on the R_{rs} Algorithm Theoretical Basis Document (ATBD) developed by the Ocean Biology Processing Group (OBPG) of the National Aeronautics and Space Administration (NASA) (OGASHAWARA *et al.*, 2020).

To correct Sentinel-2 satellite data, the ESA offers Sen2Cor (version 2.8.0), based on the ATCOR model, which determines parameters from Radiative Transfer Models calculated over the sensor type, solar geometry, terrain topography, and atmospheric parameters. More details about the SEN2COR processor and its calibration can be obtained in Main-Knorn *et al.* (2017).

For each processor, the use of default settings was defined since these are usually the best options for comparative analyses of time series in areas where atmospheric conditions are unknown (Table 1).

Tabela 1 - Similar Parameters Used During the Application of Atmospheric Correction Algorithms.

Parameter sused in atmospheric corrections	Landsat-8	Sentinel-2
Visibility*	20 km	20 km
Atmospheric Model	Tropical	Tropical
Aerosol Model	Urban	Urban
Temperature	27°C	27°C
Sensor Altitude	705 km	786 km
Sensor Type	Multispectral	Multispectral

*Note: Visibility refers to the distance at which objects can be clearly seen, often measured in kilometers. (The authors, 2023)

ISSN eletrônico 2177-2738
RA'EGA, Curitiba, PR, V.58, p. 39 – 62, 12/2023
http://dx.doi.org/10.5380/raega.v58i0.93465

It is emphasized that prior to the application of atmospheric correction algorithms, invalid pixel values, i.e., values with interference from effects such as cloud and cloud shadow, were removed. For this purpose, the Idepix plugin, integrated into the Sentinel Applications Platform (SNAP) software, was used. This facilitated the identification of invalid pixels for MSI and OLI sensors and the creation of a cloud mask to identify values that could be used and which should be excluded.

Applied Statistical Analyses

A total of 48 sample elements were collected in Paranoá Lake during field campaigns, and 28 atmospheric corrections were applied to images, considering dates and scenes from Landsat-8 and Sentinel-2 satellites. The relationships between field-observed reflectance data (reference) and surface reflectance values derived from Landsat 8 OLI and Sentinel-2 MSI sensors were analyzed using two statistical methods: Discriminant Analysis (CARVALHO *et al.*, 2020) and Covariance Analysis.

The data collected in situ were considered as independent variables, and the corrected reflectance as dependent variables. To obtain the reflectance values of pixels in the original and corrected images, the mean was calculated for each spectral band using a 3x3 window, overlapping with the field point.

First, the Kolmogorov-Smirnov test was applied, which is a non-parametric test ideal for small sample applications, without excessive restrictions, allowing measurement of the degree of agreement between the distribution of a data set and a specific theoretical distribution. In other words, it allows determining whether the samples follow a normal distribution or not. Subsequently, Pearson correlation analysis was performed to evaluate the linear relationship between field and orbital data. After confirming the data consistency, clustering techniques were applied.

Discriminant Analysis (DA) is a multivariate statistical technique and part of a predictive statistical model that has been widely used for mapping environmental variables (KRAVCHENKO *et al.*, 2002); NANNI *et al.*, 2004). This statistical method uses multivariate statistical techniques that allow separating objects from a single population—reflectance obtained from various atmospheric corrections, in the case of this study, into different classes. Hence, the choice of this method for evaluating the results obtained in the research. In addition, DA has been used to discriminate and classify specific objects or data based on the reduction of the dimensionality of data from a particular population. In other words, discriminant analysis allows determining a class association using one or more discriminant functions based on linear combinations of variables, thereby predicting the best discrimination between classes (SAPATINAS, 2005). Some studies focused on spectral data analysis have used

ISSN eletrônico 2177-2738
RA'EGA, Curitiba, PR, V.58, p. 39 – 62, 12/2023
http://dx.doi.org/10.5380/raega.v58i0.93465

this technique to classify the proximity of reflectance data collected in distinct ways (DUBE *et al.*, 2017); NYAMEKYE *et al.*, 2021).

Discriminant analysis was performed specifically for the main bands capturing the spectral response of water, including the coastal blue, blue, green, red, and near-infrared bands for Landsat-8 and Sentinel-2 sensors. The aim was to prevent outlier values from significantly impacting the analysis results. Therefore, DA was conducted as follows: for each field date and its respective image obtained through OLI and MSI sensors, analyses were conducted separately. The values of discriminant endmembers on the two main axes were then represented on a graph. This was done to allow future analysis of the accuracy and precision of each evaluated method.

To analyze the behavioral patterns between dependent and independent variables over the time span of the collected data, the Analysis of Covariance (ANCOVA) method was used. This analysis was conducted separately for each type of orbital image (Landsat-8/OLI and Sentinel-2/MSI) and for each CA algorithm used, considering all dates during the processing of each algorithm.

When statistically analyzing a specific group of data multiple times, there is a significant number of variables, and it is necessary to determine the one that will be the focus of the study, i.e., what will be the dependent variable, which in this research concerns reflectance data obtained through atmospheric corrections. The analyses were conducted separately, considering each correction algorithm and each band for all available dates. Based on these analyses, it was possible to observe which correction methods had significant differences through the Student's t-test for the identification of significant dependent variables ($Pr < 0.005$), showing variations in reflectance values over the temporal analysis window. This way, it is possible to analyze which correction algorithm and which band showed a response closest to the field data collected in situ.

III. RESULTS AND DISCUSSION

Remote Sensing and Limnological Data Analysis

The analysis of spectral curves obtained in the field with a spectroradiometer can be observed in Figure 2. It is noted that spectral curves have a similar behavior in the blue region (430 to 500nm), i.e., very low values in the main range of response for aquatic bodies in the electromagnetic spectrum. Furthermore, another important factor is the low spectral response, which is around 1%, posing a challenge for the atmospheric correction process in these studies.

ISSN eletrônico 2177-2738
RA'EGA, Curitiba, PR, V.58, p. 39 – 62, 12/2023
http://dx.doi.org/10.5380/raega.v58i0.93465

In addition to the mentioned intrinsic characteristics, it can be observed that the field data from 04/10/2020 show higher reflectance values, reaching peaks of 0.016 (1.6%) in the green region (550 to 560nm), while the other fields reached peaks of at most 1.4%, also in the green region. The spectral curves of all surveys show a region of maximum reflectance in the green between 550 and 570nm, caused by the presence of chlorophyll-a (Chl-a). The curves also exhibited an absorption feature in the red at 671nm and a reflectance peak in the near-infrared (700nm), associated with the presence of chlorophyll-a (Chl-a). Another less representative peak at 750nm is also observed, which can be attributed to the sum of scattering by phytoplankton cells and Total Suspended Solids (TSS) (KIRK, 1994; DEKKER; PETERS, 1993).

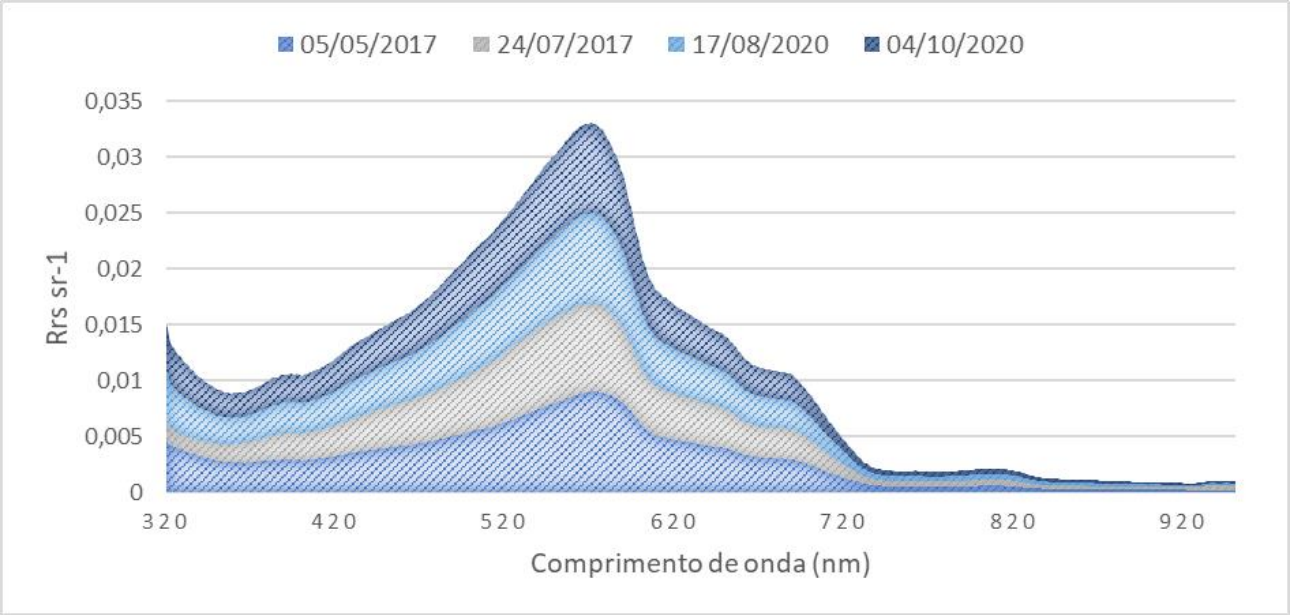

Figure 2 - Spectral curves obtained during the field campaigns. (The authors, 2023)

In this case, it can be said that despite low concentrations, there is a pattern of spectral curves showing a subtle behavior representing the presence of Chl-a (BINDING *et al.*, 2020; MACIEL *et al.*, 2019).

As illustrated in Figure 2, the mean of resampled field curves makes it clear that the spectral signatures have an ascending aspect from the blue region (430 to 500nm) to the green region (550 to 560nm) and tend to decrease subsequently, with lower values in the red region (650 to 660nm) and near-infrared (860 to 870nm). Features characteristic of the presence of Chl-a, such as the absorption feature at 670nm or the reflection at 700nm, are obscured in the generalization process performed by resampling.

Regarding orbital images, it was observed that the Landsat 8 OLI image from 04/10/2020 showed maximized reflectance values, which are due to the specular reflection effect. Despite this, the image was

ISSN eletrônico 2177-2738
RA'EGA, Curitiba, PR, V.58, p. 39 – 62, 12/2023
http://dx.doi.org/10.5380/raega.v58i0.93465

retained in the analysis to observe the effects caused in the scene through cluster analysis. The other images showed a response pattern similar to the field data.

Concerning field data, during the field campaigns, the weather conditions were favorable, with few clouds and wind conditions below the limit, except for the date of 04/10/2020. On that day, there were stronger winds, causing ripples on the water surface, making the specular reflection effect visible in the Landsat-8 Satellite image.

Limnological data obtained in the field presented in Table 2 and recent studies conducted in Lake Paranoá (BORGES *et al.*, 2020; OLIVETTI *et al.*, 2020; BARBOSA *et al.*, 2021) show that the concentration of Chl-a is very low throughout the extent of the lake. According to CONAMA resolution nº 357, the values obtained are below the established limit for the reservoir class, 30 mg/m³, indicating excellent water conditions concerning this component. Analyzing Table 2, a variation between 0.00 and 16.12 mg/l and an average of 4.83 mg/l of Chl-a are observed. For the analyzed years, based on Table 2 data, it was observed that the water meets the established standards for the reservoir for the limnological parameters measured for an oligotrophic reservoir. Regarding pH, a variation between acidic and neutral is observed, while turbidity presented concentrations below the defined limits in CONAMA resolution nº. 357 for the reservoir category. Elevated turbidity values in a reservoir can affect the photosynthetic process of the ecosystem and the entire trophic chain.

Table 2 - Summary of physical, chemical, and biological limnological variables collected in Lake Paranoá during the field campaigns of the study.

Date	Descriptive statistics	Chl-a (mg/l)	pH	Turbidity (NTU)	Temperature (°C)
05/05/2017	Mean	5,25	N/A	N/A	N/A
	Minimum	4,29	N/A	N/A	N/A
	Maximum	12,01	N/A	N/A	N/A
	SD*	2,10	N/A	N/A	N/A
24/07/2017	Mean	4,68	N/A	N/A	N/A
	Minimum	1,09	N/A	N/A	N/A
	Maximum	10,38	N/A	N/A	N/A
	SD*	2,89	N/A	N/A	N/A
17/08/2020	Mean	3,18	5,26	57,67	27,66
	Minimum	0,95	5,15	2,34	27,44
	Maximum	9,54	5,39	121,51	27,92
	SD*	1,91	0,08	44,56	0,17
04/10/2020	Mean	6,07	7,42	42,32	26,58
	Minimum	0,00	6,95	37,60	25,30
	Maximum	16,12	7,80	56,00	29,20
	SD*	4,73	0,27	5,54	0,96

*Note: SD: Standard Deviation. (The authors, 2023)

ISSN eletrônico 2177-2738
RA'EGA, Curitiba, PR, V.58, p. 39 – 62, 12/2023
http://dx.doi.org/10.5380/raega.v58i0.93465

Pearson Correlation of Field Data with Corrected Images

To assess the similarity between field data and corrected images, one of the first analyses is simple correlation. It is observed that the NIR band in all cases shows a lower correlation with field data since the field response in this region is close to zero. The blue band on both sensors showed low correlation due to the high atmospheric interference suffered in this spectral region. For the green and red bands, values tend to be highly correlated (Table 3).

For both sensors, atmospheric correction using 6S showed lower correlation with field data. The Sentinel MSI sensor had a lower correlation than that achieved by the Landsat 8 OLI sensor.

Table 3 - Pearson linear correlation between in situ Rrs and reflectances obtained through atmospheric correction and sunglint correction for each Landsat 8/OLI and Sentinel 2 MSI band.

Sensor	Band	FLAASH	6S	ACOLITE
OLI	Costal blue	-0,44	-0,56	-0,72
	B	-0,11	-0,2	-0,35
	G	0,69	0,63	0,72
	R	0,86	0,48	0,94
	NIR	0,08	-0,15	0,13
Sentinel	B	-0,81	-0,82	-0,82
	G	0,28	0,24	0,29
	R	0,25	0,09	0,23
	RedEd1	0,36	0,33	0,33
	RedEd2	0,41	0,28	0,36
	RedEd3	0,43	0,5	0,38
	NIR	0,17	0,36	0,16

(The authors, 2023)

Canonical R_{rs} Discriminant Analysis

Canonical discriminant analysis is a good tool to identify the precision and accuracy relationship of atmospheric correction algorithms. The difference in applying DA for a principal component analysis (PCA) is that in PCA, variables are rewritten as linear combinations, where each component describes a portion of the variability present in the original variables. DA, on the other hand, discriminates

When we observe the motivation for applying DA, it is understood that the analysis objectives are: 1) Dimensionality reduction for problem simplification and 2) Improvement of the ability to discriminate between classes, which in this case are the different atmospheric correction algorithms tested. Canonical correlations have the basic principle of developing a linear combination in each of the sets of variables (dependent and

ISSN eletrônico 2177-2738
RA'EGA, Curitiba, PR, V.58, p. 39 – 62, 12/2023
http://dx.doi.org/10.5380/raega.v58i0.93465

independent) such that the correlation between the two sets is maximized, indicating the quality of the discrimination of certain data based on the created discriminant axes (Fn).

According to the canonical correlations obtained by the discriminant axes, it was found that, considering the atmospheric correction algorithms applied to orbital images for each sensor and the proposed discriminant axes for all field dates, the two main axes F1 and F2 represented, at a minimum, 97% of the total information, i.e., good data discrimination quality with low point mixing. Once the data dimensionality is reduced, and these are discriminated into classes, it is possible to make certain inferences as we will comment based on Figure 3 (Landsat-8 OLI) and Figure 4 (Sentinel-2/MSI).

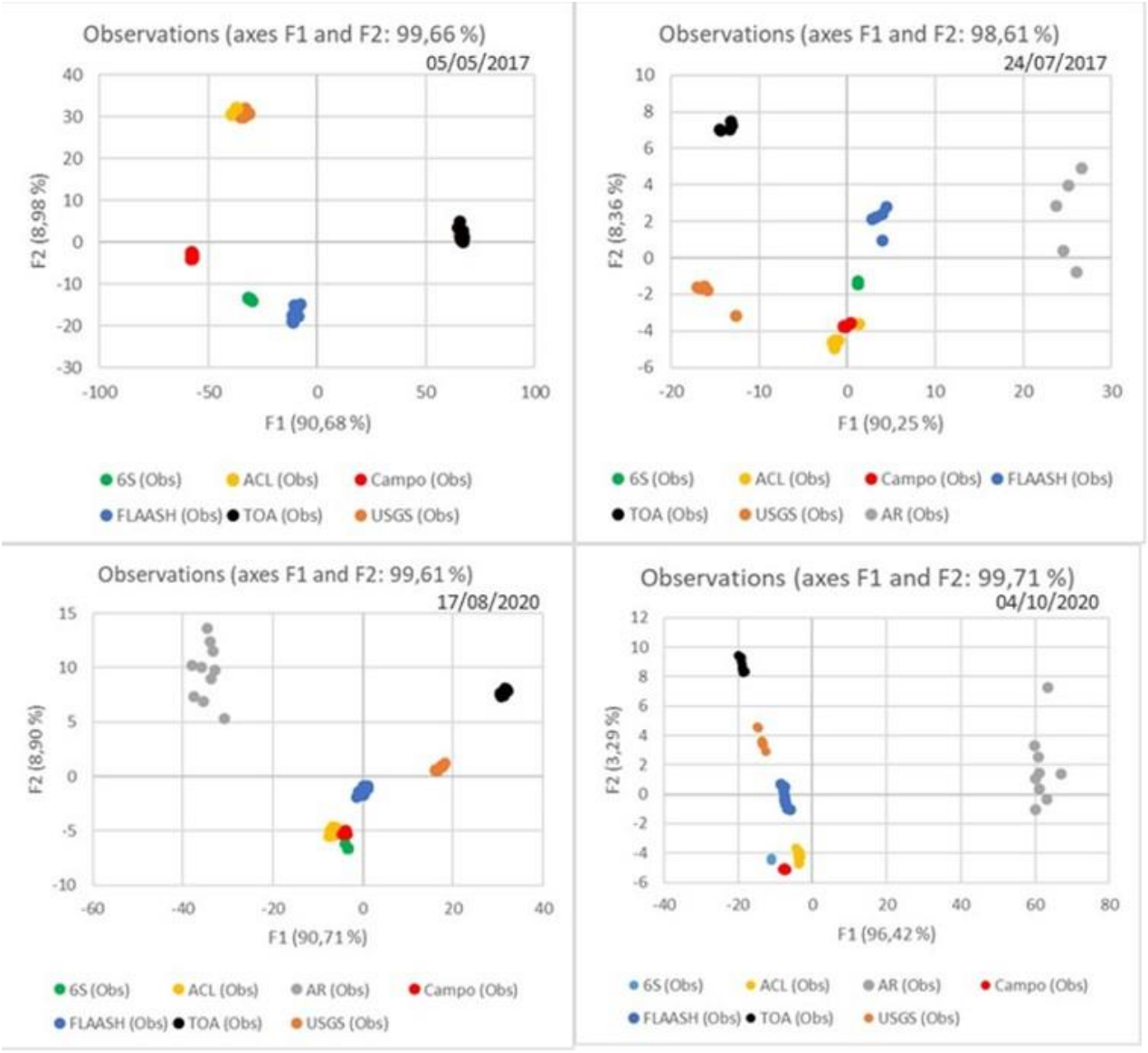

Figure 3 - Correlation of the classes obtained through Discriminant Analysis correlating the data between the main discriminant axes (F1 and F2) for the algorithms applied to images from Landsat-8/OLI on the respective field dates. AR: Aquatic reflectance; ACL: ACOLITE. (The authors, 2023)

ISSN eletrônico 2177-2738
RA'EGA, Curitiba, PR, V.58, p. 39 – 62, 12/2023
http://dx.doi.org/10.5380/raega.v58i0.93465

For the analysis in Figure 3, the proximity between surface reflectance data from orbital techniques and resampled field data (quadrant similarity and vector proximity) was considered. Regarding precision in Figure 3, it is noted that reflectance data corrected with 6S showed greater proximity to field data, although a certain homogeneity in the pattern of data dispersion compared to field data was observed. ACOLITE apparently presented a similar pattern regarding the proximity of field data, but the variability in spectral response was maintained. FLAASH, in most fields, also showed a similar pattern but with somewhat different behavior from field data. The images obtained on 2017/07/24 and 2020/10/04 were the closest to field reflectance data after the atmospheric correction process using the techniques employed by ACOLITE (ACL) and 6S.

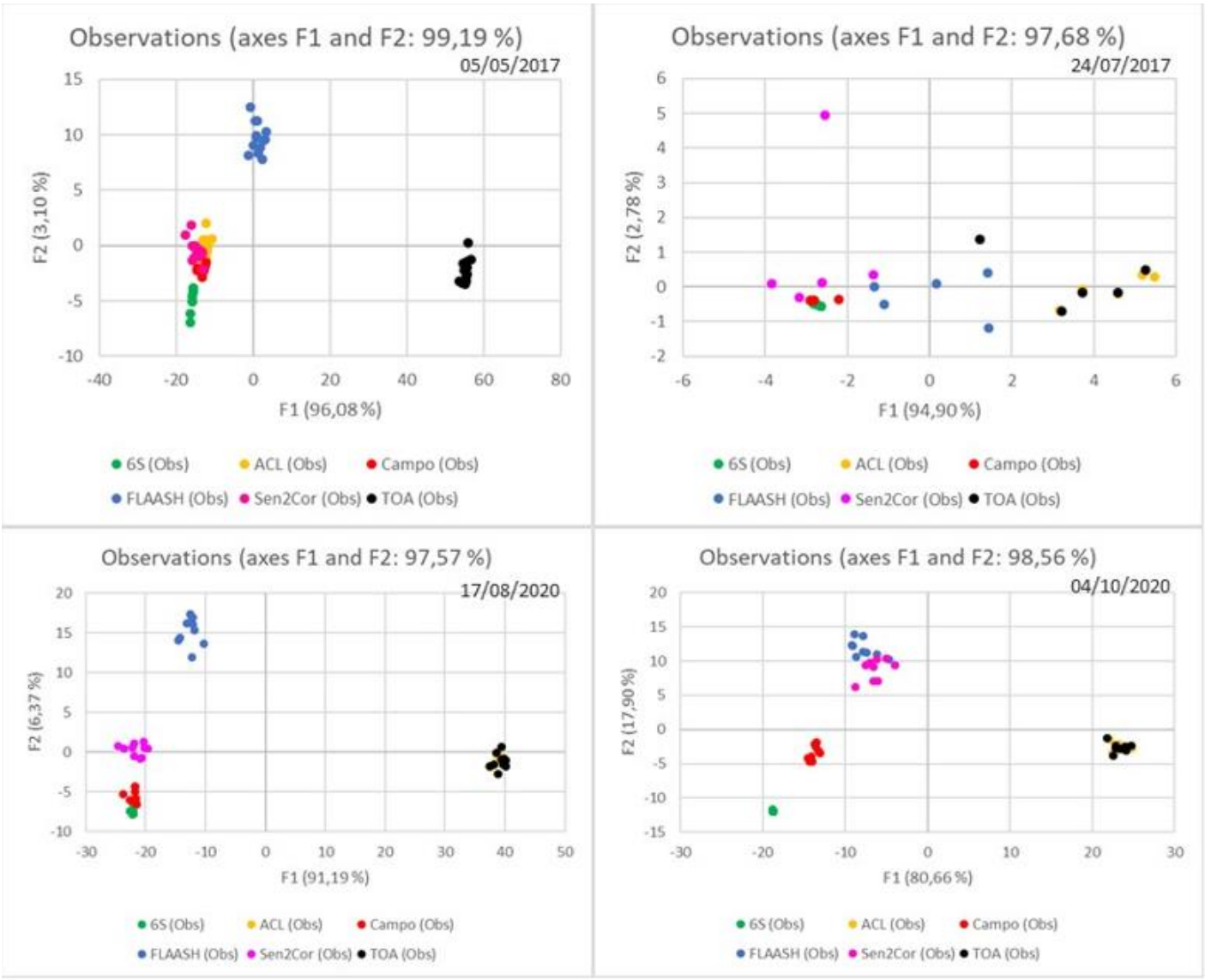

Figure 4 - Correlation of the classes obtained through Discriminant Analysis correlating the data between the main discriminant axes (F1 and F2) for the algorithms applied to images from Sentinel-2/MSI on the respective field dates. (The authors, 2023)

ISSN eletrônico 2177-2738
RA'EGA, Curitiba, PR, V.58, p. 39 – 62, 12/2023
http://dx.doi.org/10.5380/raega.v58i0.93465

The 6S presented, for all fields, similar contributions with data on both axes to data located primarily in the fourth quadrant, whose contributions on axes F1 and F2 were negative, except for the 2017/07/24 field. Regarding FLAASH data, they also had a similar behavior despite being more distant.

The TOA data showed little correlation with the field data; however, axis 1 explains a large part of the data variability. Aquatic Reflectance (AR) data exhibited high dispersion within the group, with no apparent pattern among the images (2017/07/24, 2020/0817, 2020/10/04), meaning between the analyzed axes. Thus, it is suggested that the performed correction was not able to improve the quality of water reflectance values. Ogashawara *et al.* study (2020) showed a poor relationship within situ R_{rs} for six turbid/eutrophic German lakes. The authors report that the main problem with L8PAR was the estimation of negative values for aquatic reflectance in inland waters.

For Provisional Landsat-8 Surface Reflectance Algorithm (L8SR) data, an accurate match with field data was not evident, and there was no pattern in the distribution between axes, indicating distinct information patterns between acquired images not coinciding with field data.

The 6S algorithm (Second Simulation of a Satellite Signal in the Solar Spectrum) is one of the codes that simulate radiative transfer and is widely used, with a vast amount of data and validations published over the years (VERMOTE *et al.*, 2016; EUGENIO *et al.*, 2017; YANG *et al.*, 2022; ROGER *et al.*, 2022). However, according to Pisanti *et al.* (2022), it is not capable of adequately separating and filtering the reflection that comes from the target. This characteristic, when applied in aquatic environments, needs to be considered, as these environments do not exhibit great spatial variation in R_{rs} as in terrestrial environments. It may result in the removal of atmospheric effects but also the water's response itself, so it is essential to parameterize parameters such as visibility, acquisition date and time, and sensor angle information. Thus, the physical approach is more accurate than a purely image-based approach (PISANTI *et al.*, 2022). This perception can also be indicated in the present research, given that DA indicated data with low variability after the application of this correction technique.

ACOLITE also showed significant results and has been widely used in water body applications (MACIEL; PEDOCCHI, 2022; CABALLERO *et al.*, 2022). This algorithm has the dark pixel adjustment (DSF), originally developed for applications in water bodies with high spatial resolutions but has shown high potential for Landsat-8 and Sentinel-2 images, mainly because they have the SWIR band. This band has practically zero R_{rs} response, allowing good performance if this region is not affected by adjacent effects, such as sunglint, which is corrected precisely by subtracting the SWIR band.

ISSN eletrônico 2177-2738
RA'EGA, Curitiba, PR, V.58, p. 39 – 62, 12/2023
http://dx.doi.org/10.5380/raega.v58i0.93465

However, it is important to note that the ACOLITE CA algorithm uses the ratio between R/NIR bands to correct water reflectance, which may limit its applicability to water bodies with high concentrations of Chlorophyll-a affecting absorption in the red and near-infrared regions (VANHELLEMONT, 2019; VANHELLEMONT, 2020). In other words, if Paranoá Lake did not typically have low concentrations of COAs, the algorithm's response should be reevaluated to understand the Chlorophyll-a concentration detection limit. Despite this, Ogashawara *et al.* (2020) also obtained good results for a turbid and eutrophic environment.

Figure 4 shows the classes discriminated based on atmospheric correction algorithms applied to orbital images obtained through Sentinel-2/MSI. At first glance, it is noticeable that the classes obtained by DA in atmospherically corrected MSI sensor images were not as well discriminated as for orbital images from the OLI sensor.

The precision and accuracy of the classes for this Sentinel-2/MSI sensor specifically also showed an inferior result compared to what is observed in Figure 4. Except for the 6S algorithm, which still proved more accurate than the others, even considering the Sen2Cor algorithm developed by the same company that placed the Sentinel-2/MSI satellite in orbit, the European Space Agency (ESA) (ABDELAL *et al.*, 2022). However, it is noteworthy that 6S shows a tendency towards homogeneity in the obtained reflectance data, as evidenced when compared with the behavior of the represented points of field reflectance values.

For the reflectance values obtained from atmospheric correction by ACOLITE, a variable behavior was observed between scenes and distant from the field value. It is also worth noting that the 2017/07/24 field image presented a distinct pattern from the others, with spaced and unclustered data, except for the field data and those derived from processing in 6S. TOA data closely resembled ACOLITE data for the fields of 2020/08/17 and 2020/10/04, except for the 2017/05/05 field, also showing difficulties in the atmospheric correction process.

FLAASH did not show the same performance when compared to Landsat 8 images and should be used with caution by users for atmospheric correction in Sentinel-2/MSI images.

It is important to emphasize that atmospheric correction processes followed the standard settings offered by the software, and the calibration process may reveal different behaviors in the correction process. Vanhellemont (2019), for example, reports that using an updated version of the ACOLITE processor and applying a moving average filter to the SWIR bands used for aerosol correction can help improve the quality of the results achieved. Pereira-Sandoval *et al.* (2019) report that, despite the improvement in the quality of the atmospheric correction process, Sentinel-2/MSI data showed better performance in meso- and hypereutrophic waters

ISSN eletrônico 2177-2738
RA'EGA, Curitiba, PR, V.58, p. 39 – 62, 12/2023
http://dx.doi.org/10.5380/raega.v58i0.93465

compared to oligotrophic waters, as in the environment studied in this work. The same author also states that other considerations must be considered, such as the elevation of lakes above sea level, their distance from the sea, and their morphology, which were not considered in the initial configuration of the analyzed applications.

Finally, a reflection on the effect of specular reflection (sunglint) in images must be made. The term sunglint or Sun glitter is used to denote the specific geometric condition of image acquisition that occurs specularly between the target and the remote sensor when, for a pixel or a region of the water surface, solar light is directly reflected in the line of sight of the satellite without volumetric contact with the target.

The images acquired on 2020/10/04 (Landsat OLI 8) and 2017/07/24 (Sentinel MSI) showed a pattern of response related to specular reflection, which probably reduced the effectiveness of atmospheric correction techniques. Techniques for correcting specular reflection, such as those developed by Maciel *et al.* (2019) and Harmel *et al.* (2018), should be tested before applying atmospheric correction techniques in an attempt to extract useful information from images impaired by this feature. Thus, additional and complementary studies in this direction are suggested.

Covariance Analysis of R_{rs}

The covariance analysis was applied to analyze, over time, which atmospheric correction technique can be considered part of the group of reflectance curves obtained in the field. In other words, which atmospheric correction technique was able to incorporate corrections to the point of fitting into the same group as the reference data.

As mentioned, this analysis was performed separately for each type of orbital image (Landsat-8/OLI and Sentinel-2/MSI) and for each CA algorithm used but considering all dates during the processing of each algorithm.

Since the temporal variation is now considered due to the grouping of all dates analyzed into a single series and data, it is important to ensure that in situ collected R_{rs} data (independent variable) show non-significant variation, indicating an assertive methodology for information collection, while R_{rs} data obtained by atmospheric correction should show significant values to indicate whether there is information variation detection in the time window. These analyses were obtained through the t-test, and the results of this processing are described in Table 4. It is worth noting that for data obtained through the L8PAR product, they were not considered for temporal analysis as they presented non-significant values due to their high variability.

ISSN eletrônico 2177-2738
RA'EGA, Curitiba, PR, V.58, p. 39 – 62, 12/2023
http://dx.doi.org/10.5380/raega.v58i0.93465

Considering that all field values for the CA algorithm and for the specific band did not undergo significant changes, we can consider that the data collection was carried out based on the same pattern and can be used.

For the processing applied to Landsat-8/OLI images, it is noticeable that ACOLITE obtained a better result. Considering the temporal window with the field dates during this research, the algorithm showed significant variation in the spectral responses in the Coastal Blue, Blue, Green, Red bands and was very close in the Near-Infrared (NIR) region (Table 4). This is similar to the results observed by Maciel; Pedocchi (2022) and Caballero *et al.* (2022). The 6SV algorithm was the second with significant values for some bands.

Table 4 - t-Test Values for Identifying Significant Dependent Variables (Pr < 0.005), considering the Application of Atmospheric Corrections (AC) in Landsat 8/ OLI Images

AC Algorithms	Test Pr > | t |			
	FLAASH	6S	L8SR	ACOLITE
Coastal Blue	0,715	0	0,421	0
B	0,78	0,183	0,534	0
G	0,464	0,186	0,853	0
R	0,09	0,126	0,454	0
NIR	0,63	0	0,618	0,055

(The authors, 2023)

This analysis may indicate that despite the atmospheric variations observed on different collection dates, ACOLITE was able to maintain proximity to field data in most cases, even with different images. Thus, the atmospheric correction process was able to maintain stability in atmospheric correction, following the trend of field data variance in all analyzed fields (homogeneity of regression slopes). This finding, however, cannot indicate quantitative similarity, being indicated only in the discriminant analysis technique. In other words, the result reinforces that ACOLITE can be a good alternative for handling data acquired in different images from the Landsat 8 OLI satellite.

Next, we can observe the same analysis considering the temporal window as a variable applied to the orbital images from Sentinel-2/MSI and atmospherically corrected based on the following processes (Table 5).

Table 5 - t-Test Values for Identifying Significant Dependent Variables (Pr < 0.005), considering the Application of Atmospheric Corrections (AC) in Sentinel-2/MSI Images

AC Algorithms	Test Pr > | t |		
	FLAASH	6S	ACOLITE
B	-0,81	-0,82	-0,82

ISSN eletrônico 2177-2738
RA'EGA, Curitiba, PR, V.58, p. 39 – 62, 12/2023
http://dx.doi.org/10.5380/raega.v58i0.93465

G	0,28	0,24	0,29
R	0,25	0,09	0,23
RedEd1	0,36	0,33	0,33
RedEd2	0,41	0,28	0,36
RedEd3	0,43	0,5	0,38
NIR	0,17	0,36	0,16

(The authors, 2023)

As occurred in the analyses performed for Landsat-8/OLI images, for images from Sentinel-2/MSI, field data showed non-significant values (Pr > 0.005), except for the ACOLITE CA algorithm. That is, concerning that processing and that specific sensor band, field data followed a pattern and can be used as a basis for reference data for other atmospheric correction methods.

ACOLITE is a semi-empirical method that assumes some conditions to be applied in estimating aerosol optical thickness, which are less complex than those adopted by FLAASH and 6S, for example, which are radiative transfer models (physical models), and the parameterization is more complex, bringing more input data for atmospheric characterization (YANG *et al.*, 2022).

Considering the numbers observed in Table 5, it is noticeable that the most significant values in almost all bands analyzed are the R_{rs} values obtained through the application of the 6S model. Showing that this model has significant variations, in the analyzed temporal window, for practically all studied bands.

Given the results observed, both for accuracy and precision of the data concerning in situ Rrs data, used as a reference, and for the variation of Rrs data in a specific temporal window, the 6S and ACOLITE algorithms showed better responses. Depending on the physical and chemical conditions of the target water body, the 6S and ACOLITE algorithms have been showing good responses (VANHELLEMONT, 2019; MACIEL; PEDOCCHI, 2022; CABALLERO *et al.*, 2022; YANG *et al.*, 2022).

According to Yang *et al.* (2022), who retrospectively examines the evolution of sensing for water quality analysis, physical methods have some advantages over empirical methods (high uncertainty in data) and semi-empirical methods (requires a large number of sampled points) because they do not require many field sampling points, and with a calibrated data acquisition device, there are good responses with high applicability.

ISSN eletrônico 2177-2738
RA'EGA, Curitiba, PR, V.58, p. 39 – 62, 12/2023
http://dx.doi.org/10.5380/raega.v58i0.93465

IV. CONCLUSIONS

After the application of the methodology, it became evident that atmospheric correction techniques, in their default configurations, are capable of approximating orbital reflectance values from Landsat 8 OLI and Sentinel-2 MSI satellites to field reflectance values (reference), even in oligotrophic aquatic environments.

For Landsat-8/OLI images, the 6S correction model showed both better accuracy and precision compared to other models, accompanied by the correction provided by ACOLITE. The results need to be analyzed with caution because, in principle, the 6S model, in addition to extracting information from the atmosphere, also reduced the natural spectral variability of the water body. In this case, it is understood that ACOLITE, despite being less assertive, ensured the maintenance of spectral variability.

In Sentinel-2/MSI images, it was observed initially that the classes obtained by AD atmospherically corrected were not as well discriminated as for orbital images from the OLI sensor. The 6S provided responses very similar to those obtained in the corrections of Landsat images, with the same pattern of homogenizing reflectance data. While ACOLITE was unable to ensure similarity with field data, except for the image of 2017/05.05. It is noteworthy that Sen2Cor, a technique developed by ESA itself, provided good results in terms of precision and accuracy, being recommended for this type of correction.

Images acquired on 2020/10/04 0 (Landsat 8/OLI) and 2017/07/24 (Sentinel-2/MSI) showed a pattern of response related to specular reflection, which likely reduced the effectiveness of atmospheric correction techniques. Specific correction techniques for this effect should be tested in an attempt to extract useful information from images affected by this characteristic. Thus, additional and complementary studies are suggested in this regard.

Regarding the temporal analysis, ACOLITE stood out again for Landsat-8/OLI images, followed by 6S indicating bands with responses closer to the field data collected in situ. FLAASH also performed well by ensuring significant dependent variables for some bands in the visible range. Sen2Cor presented an atypical response, which may indicate specificities in individual corrections per image. The need for additional studies is emphasized, especially for conducting analyses over time series, in addition to acquiring a greater number of field samples at different times.

Acknowledgements

This work was supported by grants from Fundação de Apoio à Pesquisa do Distrito Federal – FAP-DF (n° 00193.00001143/2021-15 and 00193-00000286/2023-71) through of the projects "Dinâmica da Qualidade da

ISSN eletrônico 2177-2738
RA'EGA, Curitiba, PR, V.58, p. 39 – 62, 12/2023
http://dx.doi.org/10.5380/raega.v58i0.93465

Água nos reservatórios do Distrito Federal (DF) por meio imagens obtidas por RPAs e por plataformas orbitais" and "Dinâmica do uso e cobertura do solo em bacias hidrográficas por meio de imagens de sensoriamento remoto e seu impacto na qualidade de água dos reservatórios de abastecimento público do DF" and by the Conselho Nacional de Desenvolvimento Científico e Tecnológico (CNPq) that granted the graduate fellowship.

V. REFERENCES

ABDELAL, Q.; ASSAF, M. N.; AL-RAWABDEH, A.; ARABASI, S.; RAWASHDEH, N. A. Assessment of Sentinel-2 and Landsat-8 OLI for Small-Scale Inland Water Quality Modeling and Monitoring Based on Handheld Hyperspectral Ground Truthing. Journal of Sensors, v. 2022, p. 1–19, 2022.

ANDERSON, G. P.; FELDE, G. W.; HOKE, M. L.; RATKOWSKI, A. J.; COOLEY, T. W.; CHETWYND J. R.; JH, ... & LEWIS. Algoritmo de correção atmosférica baseado em MODTRAN4: FLAASH (análise atmosférica de linha de visão rápida de hipercubos espectrais). In: Algoritmos e tecnologias para imagens multiespectrais, hiperespectrais e ultraespectrais VIII. SPIE, 2002. p. 65-71.

BARBOSA, C. C.; GOMES, L. N. L.; MINOTI, R. T. A modelling approach to simulate Chlorophyta and Cyanobacteria biomasses based on historical data of a Brazilian urban reservoir. Ambiente e Agua - An Interdisciplinary Journal of Applied Science, v. 16, n. 5, p. 1–11, 2021.

BATISTA, B. D.; FONSECA, B. M. Fitoplâncton da região central do Lago Paranoá (DF): uma abordagem ecológica e sanitária. Engenharia Sanitaria e Ambiental, v. 23, n. 2, p. 229–241, 2018.

BERNARDO, N.; WATANABE, F.; RODRIGUES, T.; ALCÂNTARA, E. Atmospheric correction issues for retrieving total suspended matter concentrations in inland waters using OLI/Landsat-8 image. Advances in Space Research, v. 59, n. 9, p. 2335–2348, 2017.

BERNSTEIN, L. S.; ADLER-GOLDEN, S. M.; SUNDBERG, R. L.; *et al.* Validation of the QUick atmospheric correction (QUAC) algorithm for VNIR-SWIR multi- and hyperspectral imagery. In: S. S. Shen; P. E. Lewis (Orgs.);. p.668, 2005.

BINDING, C. E.; STUMPF, R. P.; SHUCHMAN, R. A.; SAYERS, M. J. Advances in Remote Sensing of Great Lakes Algal Blooms. p.217–232, 2020.

BORGES, H. D.; CICERELLI, R. E.; DE ALMEIDA, T.; ROIG, H. L.; OLIVETTI, D. Monitoring cyanobacteria occurrence in freshwater reservoirs using semi-analytical algorithms and orbital remote sensing. Marine and Freshwater Research, v. 71, n. 5, 2020.

CABALLERO, I.; ROMÁN, A.; TOVAR-SÁNCHEZ, A.; NAVARRO, G. Water quality monitoring with Sentinel-2 and Landsat-8 satellites during the 2021 volcanic eruption in La Palma (Canary Islands). Science of The Total Environment, v. 822, p. 153433, 2022.

CARVALHO, G. A.; MINNETT, P. J.; EBECKEN, N. F. F.; LANDAU, L. Classification of Oil Slicks and Look-Alike Slicks: A Linear Discriminant Analysis of Microwave, Infrared, and Optical Satellite Measurements. Remote Sensing, v. 12, n. 13, p. 2078, 2020.

COOLEY, T.; ANDERSON, G. P.; FELDE, G. W.; *et al.* FLAASH, a MODTRAN4-based atmospheric correction algorithm, its application and validation. IEEE International Geoscience and Remote Sensing Symposium. Anais.... p.1414–1418. IEEE.

ISSN eletrônico 2177-2738
RA'EGA, Curitiba, PR, V.58, p. 39 – 62, 12/2023
http://dx.doi.org/10.5380/raega.v58i0.93465

DEKKER, A. G.; PETERS, S. W. M. The use of the Thematic Mapper for the analysis of eutrophic lakes: a case study in the Netherlands. International Journal of Remote Sensing, v. 14, n. 5, p. 799–821, 1993.

DUBE, T.; MUTANGA, O.; SIBANDA, M.; BANGAMWABO, V.; SHOKO, C. Testing the detection and discrimination potential of the new Landsat 8 satellite data on the challenging water hyacinth (Eichhornia crassipes) in freshwater ecosystems. Applied Geography, v. 84, p. 11–22, 2017.

EUGENIO, F.; MARCELLO, J.; MARTÍN, J. Multiplatform Earth Observation Systems for Monitoring Water Quality in Vulnerable Inland Ecosystems: Maspalomas Water Lagoon. Remote Sensing, v. 12, n. 2, p. 284, 2020.

EUGENIO, F.; MARCELLO, J.; MARTIN, J.; RODRÍGUEZ-ESPARRAGÓN, D. Benthic Habitat Mapping Using Multispectral High-Resolution Imagery: Evaluation of Shallow Water Atmospheric Correction Techniques. Sensors, v. 17, n. 11, p. 2639, 2017.

GONZÁLEZ-MÁRQUEZ, L. C.; TORRES-BEJARANO, F. M.; TORREGROZA-ESPINOSA, A. C.; HANSEN-RODRÍGUEZ, I. R.; RODRÍGUEZ-GALLEGOS, H. B. Use of LANDSAT 8 images for depth and water quality assessment of El Guájaro reservoir, Colombia. Journal of South American Earth Sciences, v. 82, p. 231–238, 2018.

HARMEL, T.; CHAMI, M.; TORMOS, T.; REYNAUD, N.; DANIS, P. A. Sunglint correction of the Multi-Spectral Instrument (MSI)-SENTINEL-2 imagery over inland and sea waters from SWIR bands. Remote Sensing of Environment, v. 204, p. 308–321, 2018.

DE KEUKELAERE, L.; STERCKX, S.; ADRIAENSEN, S.; *et al.* Atmospheric correction of Landsat-8/OLI and Sentinel-2/MSI data using iCOR algorithm: validation for coastal and inland waters. European Journal of Remote Sensing, v. 51, n. 1, p. 525–542, 2018.

KIRK, J. T. Light and photosynthesis in aquatic ecosystems. 1994.

KRAVCHENKO, A. N.; BOLLERO, G. A.; OMONODE, R. A.; BULLOCK, D. G. Quantitative Mapping of Soil Drainage Classes Using Topographical Data and Soil Electrical Conductivity. Soil Science Society of America Journal, v. 66, n. 1, p. 235–243, 2002.

MACIEL, D.; NOVO, E.; SANDER DE CARVALHO, L.; *et al.* Retrieving Total and Inorganic Suspended Sediments in Amazon Floodplain Lakes: A Multisensor Approach. Remote Sensing, v. 11, n. 15, p. 1744, 2019.

MACIEL, F. P.; PEDOCCHI, F. Evaluation of ACOLITE atmospheric correction methods for Landsat-8 and Sentinel-2 in the Río de la Plata turbid coastal waters. International Journal of Remote Sensing, v. 43, n. 1, p. 215–240, 2022.

MAIN-KNORN, M.; PFLUG, B.; LOUIS, J.; *et al.* Sen2Cor for Sentinel-2. In: L. Bruzzone; F. Bovolo; J. A. Benediktsson (Orgs.); Image and Signal Processing for Remote Sensing XXIII. Anais.... p.3, 2017. SPIE.

MÉLIN, F. Validation of ocean color remote sensing reflectance data: Analysis of results at European coastal sites. Remote Sensing of Environment, v. 280, p. 113153, 2022.

MOBLEY, C. D. Estimation of the remote-sensing reflectance from above-surface measurements. Applied Optics, v. 38, n. 36, p. 7442, 1999.

NANNI, M. R.; DEMATTÊ, J. A. M.; FIORIO, P. R. Análise discriminante dos solos por meio da resposta espectral no nível terrestre. Pesquisa Agropecuária Brasileira, v. 39, n. 10, p. 995–1006, 2004.

ISSN eletrônico 2177-2738
RA'EGA, Curitiba, PR, V.58, p. 39 – 62, 12/2023
http://dx.doi.org/10.5380/raega.v58i0.93465

NYAMEKYE, C.; GHANSAH, B.; AGYAPONG, E.; KWOFIE, S. Mapping changes in artisanal and small-scale mining (ASM) landscape using machine and deep learning algorithms. - a proxy evaluation of the 2017 ban on ASM in Ghana. Environmental Challenges, v. 3, p. 100053, 2021.

OGASHAWARA, I.; JECHOW, A.; KIEL, C.; *et al.* Performance of the Landsat 8 Provisional Aquatic Reflectance Product for Inland Waters. Remote Sensing, v. 12, n. 15, p. 2410, 2020.

OLIVETTI, D.; ROIG, H.; MARTINEZ, J. M.; *et al.* Low-Cost Unmanned Aerial Multispectral Imagery for Siltation Monitoring in Reservoirs. Remote Sensing, v. 12, n. 11, p. 1855, 2020.

PASSOS, M. C. DOS; RIBEIRO, F. P.; TEIXEIRA, T. M. DE A.; VALADÃO, M. B. X. Crise hídrica no Distrito Federal, Brasil: uma visão acadêmica. Research, Society and Development, v. 9, n. 11, p. e1139119518, 2020.

PEREIRA-SANDOVAL, M.; RUESCAS, A.; URREGO, P.; *et al.* Evaluation of Atmospheric Correction Algorithms over Spanish Inland Waters for Sentinel-2 Multi Spectral Imagery Data. Remote Sensing, v. 11, n. 12, p. 1469, 2019.

PISANTI, A.; MAGRÌ, S.; FERRANDO, I.; FEDERICI, B. SEA WATER TURBIDITY ANALYSIS FROM SENTINEL-2 IMAGES: ATMOSPHERIC CORRECTION AND BANDS CORRELATION. The International Archives of the Photogrammetry, Remote Sensing and Spatial Information Sciences, v. XLVIII-4/W1-2022, p. 371–378, 2022.

ROGER, J. C.; VERMOTE, E.; SKAKUN, S.; *et al.* Aerosol models from the AERONET database: application to surface reflectance validation. Atmospheric Measurement Techniques, v. 15, n. 5, p. 1123–1144, 2022.

SAPATINAS, T. Discriminant Analysis and Statistical Pattern Recognition. Journal of the Royal Statistical Society Series A: Statistics in Society, v. 168, n. 3, p. 635–636, 2005.

STEINMETZ, F.; DESCHAMPS, P.-Y.; RAMON, D. Atmospheric correction in presence of sun glint: application to MERIS. Optics Express, v. 19, n. 10, p. 9783, 2011.

VANHELLEMONT, Q. Adaptation of the dark spectrum fitting atmospheric correction for aquatic applications of the Landsat and Sentinel-2 archives. Remote Sensing of Environment, v. 225, p. 175–192, 2019.

VANHELLEMONT, Q. Sensitivity analysis of the dark spectrum fitting atmospheric correction for metre- and decametre-scale satellite imagery using autonomous hyperspectral radiometry. Optics Express, v. 28, n. 20, p. 29948, 2020.

VANHELLEMONT, Q.; RUDDICK, K. Advantages of high quality SWIR bands for ocean colour processing: Examples from Landsat-8. Remote Sensing of Environment, v. 161, p. 89–106, 2015.

VERMOTE, E.; JUSTICE, C.; CLAVERIE, M.; FRANCH, B. Preliminary analysis of the performance of the Landsat 8/OLI land surface reflectance product. Remote Sensing of Environment, v. 185, p. 46–56, 2016.

WANG, D.; MA, R.; XUE, K.; LOISELLE, S. The Assessment of Landsat-8 OLI Atmospheric Correction Algorithms for Inland Waters. Remote Sensing, v. 11, n. 2, p. 169, 2019.

WANG, Z.; XIA, J.; WANG, L.; *et al.* Atmospheric Correction Methods for GF-1 WFV1 Data in Hazy Weather. Journal of the Indian Society of Remote Sensing, v. 46, n. 3, p. 355–366, 2018.

WARREN, M. A.; SIMIS, S. G. H.; MARTINEZ-VICENTE, V.; *et al.* Assessment of atmospheric correction algorithms for the Sentinel-2A MultiSpectral Imager over coastal and inland waters. Remote Sensing of Environment, v. 225, p. 267–289, 2019.

ISSN eletrônico 2177-2738
RA'EGA, Curitiba, PR, V.58, p. 39 – 62, 12/2023
http://dx.doi.org/10.5380/raega.v58i0.93465

YANG, H.; KONG, J.; HU, H.; *et al.* A Review of Remote Sensing for Water Quality Retrieval: Progress and Challenges. Remote Sensing, v. 14, n. 8, p. 1770, 2022.